

Adaptation to hypoxia in the diabetic rat kidney

C Rosenberger¹, M Khamaisi^{2,3}, Z Abassi⁴, V Shilo², S Weksler-Zangen³, M Goldfarb⁵, A Shina², F Zibertrest², K-U Eckardt⁶, S Rosen⁷ and SN Heyman²

¹Nephrology and Medical Intensive Care, Charité University Clinic, Berlin, Germany; ²Departments of Medicine, Hadassah Hospitals, Mt Scopus and Ein Kerem and the Hebrew University Medical School, Jerusalem, Israel; ³Diabetes Research Unit, Hadassah Hospital, Ein Kerem and the Hebrew University Medical School, Jerusalem, Israel; ⁴Department of Physiology, Technion Medical School, Haifa, Israel; ⁵Nephrology Unit, Bikur Holim Hospital, Jerusalem, Israel; ⁶Department of Nephrology and Hypertension, University of Erlangen-Nuremberg, Erlangen, Germany and ⁷Department of Pathology, Beth Israel Deaconess Medical Center and Harvard Medical School, Boston, Massachusetts, USA

Hypoxia of the kidney in diabetes could predispose it to develop acute and chronic renal failure. To examine the relationship between renal hypoxia and renal failure, we measured hypoxia (as a pimonidazole adducts), hypoxia-inducible factors (HIFs), and a hypoxia target gene heme oxygenase-1. The studies were performed in rats with streptozotocin (STZ)-induced diabetes, Cohen diabetes sensitive rats, and during short-term artificial hyperglycemia in rats induced by intravenous glucose and octreotide. STZ-treated rats received insulin, the superoxide dismutase mimetic tempol, or contrast medium. Radiocontrast media causes hypoxia and HIF induction. Hypoxia, HIFs, and heme oxygenase were undetectable in controls, but transiently activated in STZ-treated and the Cohen diabetes sensitive rats. Different patterns of HIFs and pimonidazole were observed between the three models. Insulin abolished pimonidazole and HIF induction, whereas tempol lead to increased HIFs and heme oxygenase induction at similar levels of pimonidazole. When compared with control rats, STZ-treated rats exhibited more intense and protracted renal pimonidazole, with augmented hypoxia inducible factor production and reduced GFR following contrast media. Our data suggest that both regional hypoxia and hypoxia adaptation transiently occur in early stages of experimental diabetes, largely dependent on hyperglycemia or after contrast media. Tempol may augment the HIF response in diabetes.

Kidney International (2008) **73**, 34–42; doi:10.1038/sj.ki.5002567; published online 3 October 2007

KEYWORDS: hypoxia; diabetes mellitus; heme oxygenase; immunohistochemistry; cell biology; renal pathology

Correspondence: C Rosenberger, Nephrology and Medical Intensive Care, Charité Universitaetsmedizin, Augustenburger Platz 1, Berlin 13353, Germany. E-mail: chrosenbe@aol.com

Received 2 February 2007; revised 6 July 2007; accepted 7 August 2007; published online 3 October 2007

To our knowledge, there is no generally accepted definition of hypoxia. Hochachka *et al.*¹ have nicely reviewed how cells reduce their ATP production and consumption, when 'oxygen availability becomes limiting', a paraphrase of the term 'hypoxia'. Obviously, they understand 'hypoxia' as a condition which elicits either cell damage or specific adaptational responses, termed 'hypoxia adaptation'. In this study hypoxia is considered as a pathologic condition of mismatch between oxygen supply and consumption. Accordingly, in the normal kidney, oxygen homeostasis would be preserved. This would be in line with the fact that in our hands the hypoxia detection tools employed in this study, namely pimonidazole adducts (PIM) and hypoxia-inducible factors (HIFs), are hardly detectable or undetectable in normal kidneys, despite known low pO₂ within the renal medulla.

Recently, using oxygen microelectrodes, Palm *et al.*² found that renal tissue pO₂ is substantially lower in diabetic rats, as compared with control (CTR) animals. Using blood oxygen level-dependent magnetic resonance imaging Ries *et al.*³ have shown that deoxyhemoglobin signals rose in the diabetic kidney, particularly in the outer medullary region. Intrarenal microcirculation was not altered,² whereas oxygen consumption *ex vivo* by cortical and medullary tubular cells was significantly enhanced.² Taken together these data suggest that the diabetic kidney is more likely to develop hypoxia.

Increasing evidence suggests that regional renal hypoxia plays an important pathophysiologic role in acute kidney injury (AKI), irrespective of the underlying cause.^{4,5} Furthermore, chronic hypoxia seems to play an important role in the progression of chronic renal failure.⁶ Thus, evaluation of renal hypoxia could be important for the understanding of AKI and CRF in diabetes. Indeed, diabetes is a major risk factor for the development of specific subsets of AKI, namely papillary necrosis,⁷ contrast nephropathy,^{8,9} and or following cardiac bypass operations,^{10,11} and is becoming the leading cause of end-stage kidney disease in developed countries.¹²

Hypoxia adaptation takes place within the kidney, conferred through HIFs. HIFs are heterodimers composed of a constitutive β -subunit and one of at least two different

oxygen-dependent α -subunits. Regulation of HIF mainly occurs by oxygen-dependent proteolysis of the α -subunit. HIFs govern transcriptional activity of a host of genes, many of which are cell/tissue protective.¹³⁻¹⁶ Yet, HIF may also exert adverse responses, such as the aggravation of diabetic retinopathy through the induction of vascular endothelial growth factor.¹⁷

HIF activity can be modulated by a number of factors, among which are reactive oxygen species (ROS) like hydrogen peroxide and superoxide (O_2^-).¹⁸⁻²¹ Diabetes leads to increased production of ROS.²² In the renal medulla, thick ascending limbs of the loop of Henle (TALs) produce O_2^- due to increased NAD(P)H oxidase activity.²³ O_2^- has been shown to induce renal vascular constriction,²⁴ to enhance tubular salt reabsorption,²⁵ and reduce HIF activity.²⁶ Hence, O_2^- may both intensify renal medullary hypoxia and reduce hypoxia adaptation in diabetes. The soluble cell membrane-permeable superoxide dismutase mimetic tempol has been shown to reduce O_2^- levels *in vivo*,²⁷ but its effect on renal medullary hypoxia has not been assessed in diabetes, so far. The cell-protective effect of the HIF target gene heme oxygenase-1 (HO-1) relies, at least partly, on its ROS scavenging ability.²⁸ Therefore, HO-1 activation may protect from diabetes-induced renal injury.

This study was designed to explore the cellular and temporal distribution and the underlying mechanisms of renal hypoxia in experimental diabetes, to identify potential hypoxia adaptation, and to assess the possible relationship between renal hypoxia and susceptibility to AKI in diabetes.

RESULTS

Functional parameters after induction of diabetes

Rats with streptozotocin (STZ)-induced diabetes developed both fasting and postprandial (PP) hyperglycemia (Glc)

within 2 days (393 ± 35 mg dl⁻¹) as compared with 88 ± 2 mg dl⁻¹ in CTRs) (Table 1). Plasma insulin (37 ± 5 μ U ml⁻¹ in CTR) determined at 2, 7, and 14 days of STZ was significantly reduced to 18 ± 2 μ U ml⁻¹, 21 ± 2 , and 25 ± 1 μ U ml⁻¹ ($n = 4$ per group, $P < 0.01$ vs CTR). At 14–90 days of STZ, kidney/body weight ratio, urine volume, plasma urea, kaliuresis, and weight-adjusted creatinine clearance were all significantly elevated, whereas animal weight and tubular sodium reabsorption were significantly depressed.

Cohen diabetes sensitive rats (CDS rats) kept on a diabetogenic diet for 30 days had normal fasting glucose, but prolonged PP hyperglycemia (Glc). When compared with rats 30 days after STZ, animal weight was higher, whereas weight-adjusted creatinine clearance, PP glycemia, and urine volume were lower.

PIM, HIFs, and HO-1 transiently occur in diabetic rats

PIM were detectable as early as 7 days after STZ injection, increased at 14 and 30 days (papilla and inner stripe of the outer medulla), but were no longer present at 90 days. Potential hypoxia-adaptive response, manifested by HIF and HO-1 expression, closely followed; PIM, HIF-1 α , HIF-2 α , and the HIF target gene HO-1 all located in the same renal zones, mostly within 2 to 5 tubular diameters distance (Figures 1 and 2; Table 2). Noteworthy, most likely HIFs and PIM have different kinetics and different hypoxia thresholds, and activation of HIF target gene products occurs with a delay of several hours. Not surprisingly, PIM, HIF, and HO-1 signals showed only partial overlap at the cellular level, as has been observed in previous studies.²⁹⁻³¹ Evidence of hypoxia was confined to the inner stripe of the outer medulla (Figure 1) and the papilla (Figure 2). As previously described in other experimental models,²⁹⁻³¹ HIF-1 α appeared in

Table 1 | Functional changes in diabetic rats

	CTR-2 (7 days) (n=11)	STZ (2 days) (n=8) ^a	STZ (7 days) (n=8) ^a	CTR-14-30 days (n=46)	STZ (14 days) (n=35) ^b	STZ (30 days) (n=7) ^b	CTR(90 days) (n=9)	STZ (90 days) (n=8) ^c	CDS-rats (30 days) (n=10) ^d
Body weight (g)	280 ± 8	291 ± 20	248 ± 12 ^e	345 ± 3	268 ± 17 ^f	231 ± 24 ^f	406 ± 5	234 ± 9 ^f	235 ± 7
Two kidney weight (g)	3.0 ± 0.1	3.3 ± 0.3	2.9 ± 0.1	3.1 ± 0.1	3.6 ± 0.2 ^g	3.7 ± 0.4	3.7 ± 0.2	3.5 ± 0.1	2.6 ± 0.1 ^g
Kidney/body weight (%)	0.9 ± 0.0	1.0 ± 0.0	1.0 ± 0.0	0.9 ± 0.0	1.2 ± 0.1 ^g	1.6 ± 0.1 ^f	0.9 ± 0.0	1.6 ± 0.1 ^f	1.1 ± 0.0 ^f
Blood glucose (mg dl ⁻¹)	88 ± 2	393 ± 35 ^f	384 ± 22 ^f	91 ± 3	394 ± 11 ^f	380 ± 29 ^f	87 ± 6	415 ± 26 ^f	252 ± 33 ^g
Urine volume (ml h ⁻¹)	0.5 ± 0.0	ND	ND	0.5 ± 0.0	5.5 ± 0.4 ^f	3.4 ± 0.7 ^f	0.6 ± 0.1	3.3 ± 0.4 ^f	0.7 ± 0.1 ^f
PCr (μ mol l ⁻¹)	53 ± 5	ND	ND	51 ± 1	49 ± 2	46 ± 3	51 ± 0	38 ± 3 ^e	55 ± 2 ^e
P-urea (mmo l ⁻¹)	7.0 ± 0.2	ND	ND	6.6 ± 0.2	11.0 ± 0.8 ^f	16.9 ± 5.3 ^f	7.3 ± 0.5	14.9 ± 2.3 ^f	6.0 ± 0.6 ^e
Cl _{Cr} (ml min ⁻¹) (ml min ⁻¹ 100 g ⁻¹)	1.1 ± 0.1	ND	ND	1.5 ± 0.1	1.9 ± 0.1 ^e	1.8 ± 0.4	1.5 ± 0.3	1.4 ± 0.1	0.6 ± 0.3 ^g
TRNa (%)	0.4 ± 0.0	ND	ND	0.4 ± 0.0	0.6 ± 0.0 ^f	0.8 ± 0.2 ^f	0.4 ± 0.1	0.6 ± 0.1 ^e	0.3 ± 0.0 ^g
TRNa (%)	99.5 ± 0.0	ND	ND	99.7 ± 0.1	99.0 ± 0.1 ^f	99.1 ± 0.2 ^e	99.5 ± 0.1	99.0 ± 0.3 ^g	96.9 ± 2.7
FEK (%)	16.5 ± 8.5	ND	ND	9.3 ± 1.1	38.7 ± 1.7 ^f	21.4 ± 4.1 ^e	11.3 ± 3.9	24.8 ± 4.4 ^g	21.2 ± 2.1

CDS rats, Cohen diabetes sensitive rats; Cl_{Cr}, creatinine clearance; CTR, control; FEK, fractional potassium excretion; ND, not determined; PCr, plasma creatinine; STZ, streptozotocin; TRNa, tubular sodium reabsorption.

^aTested vs CTR-2–7 days.

^bTested vs CTR-14–30 days.

^cTested vs CTR-90 days.

^dTested vs STZ-30 days.

^e $P < 0.05$.

^f $P < 0.001$ vs respective control group, 1-way ANOVA.

^g $P < 0.01$.

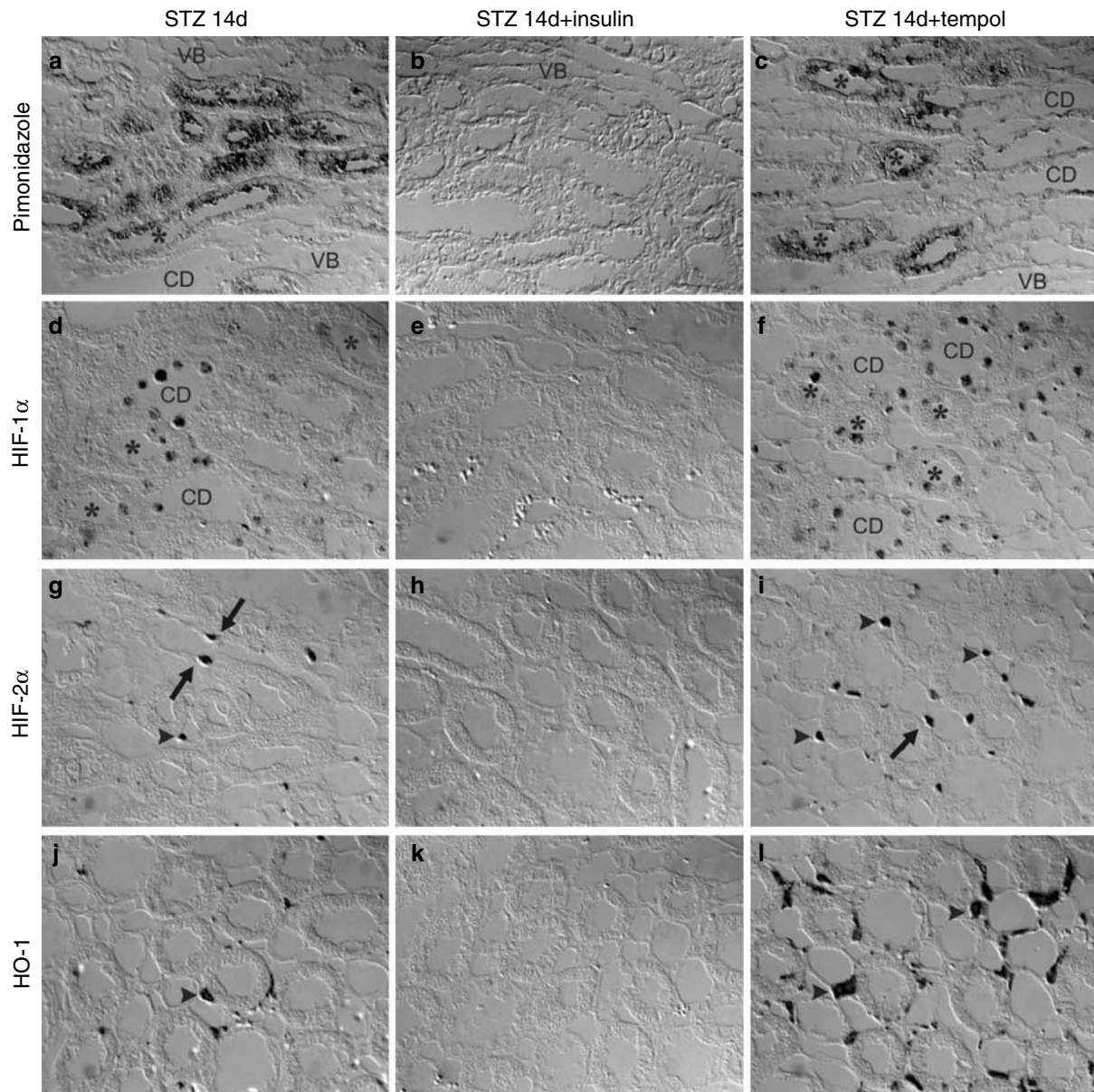


Figure 1 | PIM, HIFs and HO-1 in the inner stripe of the outer medulla in STZ-induced diabetes. Immunohistochemistry for the hypoxia marker pimonidazole (PIM), HIF-1 α , HIF-2 α , and the HIF target gene HO-1; asterisk = thick ascending limb (TAL), CD = collecting duct; arrow = endothelial cell; arrowhead = interstitial cell; STZ = streptozotocin, VB = vascular bundles. Rats were studied at 14 days of STZ. No signals for either marker were detected in non-diabetic CTRs (not shown). PIM occurred in TALs and to a lesser extent in CDs, increasing with distance from VBs (a). HIF-1 α appeared in CDs and TALs (d), whereas HIF-2 α appeared in capillary endothelial cells and in the interstitial cells of the inter-bundle zone (g). The HIF target gene HO-1 was detected in interstitial cells (j). Two days of treatment abolished renal PIM and HIFs (b, e, h, k). Twelve days of treatment with the superoxide dismutase mimetic tempol had no major effect on PIM (c), but HIF-1 α (f), HIF-2 α (i), and HO-1 (l) were increased. Magnifications: (a-c), $\times 440$; (d-l), $\times 600$.

tubules and in papillary interstitial cells, whereas HIF-2 α exclusively located in non-epithelial cells (Figures 1 and 2). In the inner stripe of the outer medulla, HIF-1 α signals were present in both medullary thick ascending limbs (mTALs) and collecting ducts (CDs) (Figure 1d). This pattern of tubular HIF-1 α expression contrasts with previous studies, using different hypoxic stimuli, in which HIF-1 α has almost exclusively been detected in CDs in this particular renal zone.^{29–32} HO-1 appeared in outer medullary interstitial cells (Figure 1j). Signal density/intensity increased toward

the mid-inter-bundle zone (away from oxygen supplying vasa recta, not shown), suggesting hypoxic induction of HO-1.

Since STZ rats conceivably was hypovolemic, a condition that *per se* can induce renal hypoxia,³³ additional animals received fluids at 14 days of STZ, but the HIF/PIM/HO-1 signals remained unaffected (Table 2). Moreover, in CDS rats, in which fluid balance was better maintained, the signals for PIM, HIFs, and HO-1 were of similar distribution and extent as in STZ (Table 3).

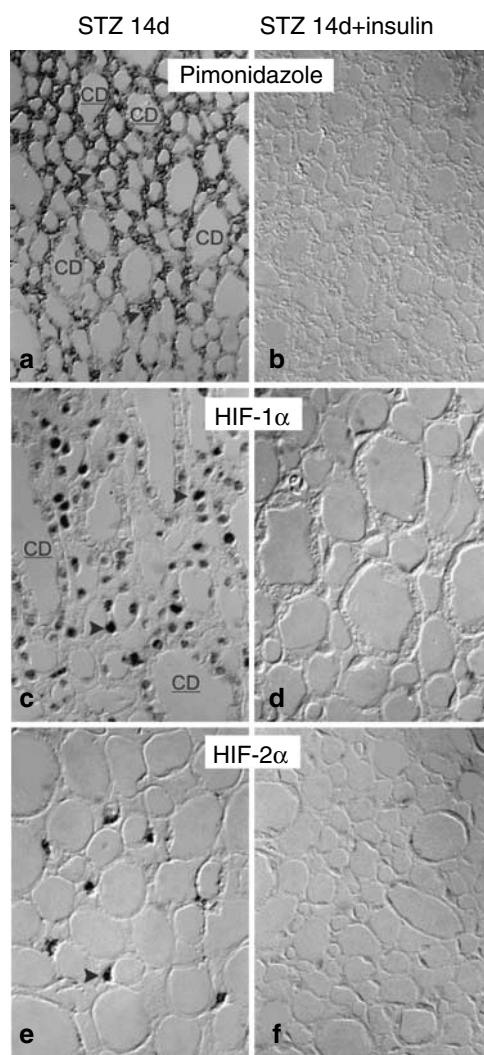


Figure 2 | PIM and HIFs in the papilla in STZ-induced diabetes. Immunohistochemistry for the hypoxia marker pimonidazole (PIM), HIF-1 α , and HIF-2 α ; CD = unstained collecting duct; CD = stained collecting duct; arrowhead = interstitial cell; STZ = streptozotocin. Rats were studied at 14 days of STZ. No signals for either marker were detected in non-diabetic CTRs (not shown). PIM occurred in all cellular compartments in the core of the papilla (upper portion in **a**). However, toward the papillary tip (lower portion in **a**), CDs became negative for PIM, whereas some interstitial staining was preserved. HIF-1 α mainly appeared in CDs and interstitial cells (**c**), whereas HIF-2 α mainly appeared in interstitial cells (**e**). Two days of insulin treatment abolished renal papillary PIM and HIFs (**b**, **d**, **f**). Magnifications: (**a**, **b**), $\times 440$; (**c-f**), $\times 600$.

PIM and HIF-2 are activated in artificial hyperglycemia

To test whether hyperglycemia *per se* augments renal medullary PIM and activates HIF, we induced artificial hyperglycemia (Glc) in three CTR rats, with the help of glucose and octreotide infusion, and determined hypoxia markers after 2 h of sustained Glc (380–465 mg dl⁻¹). Indeed, PIM was detectable in the papillary interstitium (Figure 3). This pattern differed from that observed in both STZ and CDS rats. In the latter two both interstitial and tubular elements stained for PIMs. Noteworthy, in Glc tubular compartments

were HIF-1 α negative. By contrast, HIF-2 α appeared in endothelial cells in all renal zones (Table 3).

Insulin treatment abolishes PIM and HIFs in STZ

To test whether glycemic CTR could ameliorate renal hypoxia, additional animals received insulin implants at 12–14 days of STZ, with fasting glucose declining to 55 ± 8 mg dl⁻¹. Kidneys were negative for either PIM or HIFs, suggesting that oxygen homeostasis had been restored (Figures 1 and 2; Table 2).

Tempol has no major impact on renal PIM, but enhances HIFs and HO-1 in STZ

To determine the possible contribution of O₂⁻ (which is increased in diabetic kidneys²²) to the genesis of renal medullary hypoxia, the soluble superoxide dismutase mimetic, tempol, was delivered to STZ rats from 2–14 days after the induction of diabetes. Tempol led to a statistically non-significant trend ($P = 0.075$) for less PIM in the inner stripe of the outer medulla (Figure 1; Table 2), or in the papilla (Table 2). Tempol markedly increased HIF-1 α , HIF-2 α , and the HIF target gene HO-1 in the inner stripe of the outer medulla (but not in the papilla, not shown; Figure 1; Table 2).

Diabetes enhances contrast medium-induced renal medullary PIM and HIFs

Since renal medullary PIM and HIF α activation,²⁹ as well as enhanced deoxyhemoglobin,³⁴ have been shown at 2 h after the injection of contrast medium (CM) in CTR rats, we sought to examine whether CM would intensify PIM and HIFs in diabetic kidneys. In addition, since diabetes predisposes to CM-induced nephropathy,^{8,9} we determined renal function and tubular damage (in 1 μ m semi-thin plastic sections) at 24 h after CM. Diabetic animals used in these studies were at 14 days of STZ. No major tubular damage was evident in either experimental group, but creatinine clearance significantly dropped in STZ, while being stable in CTR (Table 4).

Moreover, the extent and time course of PIM and HIFs appearance were different between CTR and diabetic rats (Table 5). In CTR rats PIM transiently occurred at 1 h, being undetectable at baseline and at 2 h, respectively. HIFs were absent at baseline, upregulated at 1 h, and less prominent but still detectable at 2 h. By contrast, in STZ both PIM and HIFs were already evident at baseline, markedly intensified at 1 h, and sustained at 2 h. Our results suggest that in diabetes, CM-induced renal medullary hypoxia is intensified and protracted.

To exclude that the functional changes observed after CM were, at least partly, caused by STZ nephrotoxicity (which has been reported up to 3 weeks after its administration³⁵), we injected CM at 30 days of STZ ($n = 8$), as well as in age-matched CTRs ($n = 8$). Again, in STZ, creatinine clearance significantly dropped (0.66 ± 0.17 mg ml⁻¹ · 100 g at baseline vs 0.45 ± 0.09 mg ml⁻¹ · 100 g at 1 day, $P < 0.05$), whereas it remained stable in CTR (0.33 ± 0.03 mg ml⁻¹ · 100 g at

Table 2 | PIM, HIFs, and HO-1 in experimental diabetes along time (inner stripe of the outer medulla)

	STZ									CDS rats 30 days
	CTR	2 days	7 days	14 days			30 days	90 days		
				+tempol	+insulin	+fluid				
<i>n</i>	5	4	4	13	5	7	3	6	4	5
PIM	0	0	0.7 ± 0.3	2.3 ± 0.2 ^a	1.6 ± 0.2	0.3 ± 0.2 ^b	2.0 ± 0.0	2.0 ± 0.0 ^a	0	2.0 ± 0.3
HIF-1 α	0	0	0.5 ± 0.3	1.8 ± 0.2 ^a	3.2 ± 0.4 ^b	0.4 ± 0.2 ^b	2.0 ± 0.0	2.0 ± 0.3 ^a	0	2.2 ± 0.4
HIF-2 α	0	0	0.5 ± 0.3	1.8 ± 0.2 ^a	2.8 ± 0.2 ^c	0.3 ± 0.2 ^b	1.7 ± 0.3	1.6 ± 0.2 ^a	0	1.8 ± 0.2
HO-1	0	0	1.0 ± 0.4 ^d	1.9 ± 0.2 ^a	3.2 ± 0.8 ^e	0.4 ± 0.2 ^b	1.7 ± 0.3	1.6 ± 0.2 ^a	0	1.4 ± 0.2

CTR, non-diabetic control; CDS rats, Cohen diabetes sensitive rats; HIF, hypoxia-inducible factor; HO-1, heme oxygenase-1; PIM, pimonidazole adduct; STZ, streptozotocin. Semiquantitative immunohistochemical staining: 0, no signals detectable; 1+, staining in <5% of tubular profiles or interstitial/endothelial cells; 2+, 5–20%; 3+, 20–33%. Irrespective of the experimental condition, location of signals followed the same renal zone-specific pattern (see Table 4).

^a*P* < 0.001.

^b*P* < 0.001.

^c*P* < 0.01.

^d*P* < 0.05, vs CTR.

^e*P* < 0.05 vs STZ 14 days, ANOVA.

Table 3 | Different location of PIM, HIFs, and HO-1 in experimental diabetes vs artificial Glc

	Pimonidazole		HIF-1 α		HIF-2 α	
	Diabetes STZ (14 days)	Artificial hyperglycemia	Diabetes STZ (14 days)	Artificial hyper-glycemia	Diabetes STZ (14 days)	Artificial hyper-glycemia
Cortex	—	—	—	—	—	EC _{gr} , EC _{ti}
Outer stripe	—	—	—	—	—	EC _{ti}
Inner stripe	TAL	—	TAL	—	EC _{ti} , IC	EC _{vb}
Papilla	CD, IC, EC, ECM	IC (ECM)	CD, IC	—	EC, IC	EC (IC)

CD, collecting duct; EC, endothelial cell; EC_{gr}, glomerular EC; EC_{ti}, tubulo-interstitial EC; EC_{vb}, vascular bundle EC; ECM, extracellular matrix; Glc, hyperglycemia; HIF, hypoxia-inducible factor; IC, interstitial cell; inner stripe, inner stripe of the outer medulla; outer stripe, outer stripe of the outer medulla; STZ, streptozotocin; TAL, thick ascending limb.

baseline vs $0.32 \pm 0.02 \text{ mg ml}^{-1} \cdot 100 \text{ g}$ at 1 day). Rare focal mTAL damage (<1% of tubules in the mid-inner stripe) was noted in 2/8 of the diabetic animals but not in the CTR group.

DISCUSSION

This study reveals following five main findings: first, renal medullary PIM and HIFs occur in experimental models of insulin-deficient diabetes, suggesting renal hypoxia; second, diabetic renal hypoxia likely is dependent on Glc, since it is prevented by short-term insulin treatment; third, diabetes and artificial Glc elicit different renal hypoxia patterns, suggesting a contribution of diabetes-induced morpho-functional changes to renal hypoxia; fourth, the superoxide dismutase mimetic tempol enhances HIFs and the HIF target gene HO-1 in diabetes; and fifth, after CM, diabetic renal medullary PIM and HIFs are enhanced, suggesting intensified and protracted hypoxia.

To our knowledge, this is the first immunohistochemical report of both PIM and HIFs in the diabetic kidney. Using PIM immunostaining, we confirm a reduced oxygen content in the diabetic renal medulla, previously shown by oxygen electrode and blood oxygen level-dependent magnetic resonance imaging measurements in STZ diabetes.^{2,3} We validate these findings, eliminating a possible effect of STZ itself, showing a similar pattern of distribution of PIM adducts in CDS rats. Our results further suggest that a

pathologic hypoxic condition (hence termed ‘hypoxia’ for simplicity) occurs in the diabetic renal medulla, since HIFs and HO-1 are activated, indicating hypoxia adaptation. This study extends previous data by assigning hypoxia and potential hypoxia adaptation to particular cellular elements.

Possible mechanisms of diabetes-induced renal hypoxia

The mechanism(s) responsible for the transient occurrence of renal hypoxia in early experimental diabetes most likely relates to increased tubular oxygen consumption for salt reabsorption. Consistent with mTAL workload being a major determinant of outer medullary oxygenation,³⁶ PIM was mostly detected in mTALs. Moreover, insulin treatment, which abolished hypoxia markers in this study, could have reduced tubular workload both by glomerular filtration rate reduction³⁷ and the amelioration of osmotic diuresis. The latter mechanism has been shown to reduce early distal tubular NaCl content, which is consistent with increased sodium reabsorption of the preceding nephron segments.³⁸

Short-term (2 h) Glc was sufficient to induce the ‘complete’ PIM/HIF pattern in CDS rats (which have normal fasting blood glucose and were studied at 2 h after food intake). But 2 h of artificial Glc in Sprague-Dawley (SD) rats produced a different and somehow ‘incomplete’ PIM/HIF pattern, when compared with STZ/CDS rats. Most likely, morpho-functional changes (e.g., tubular hypertrophy,

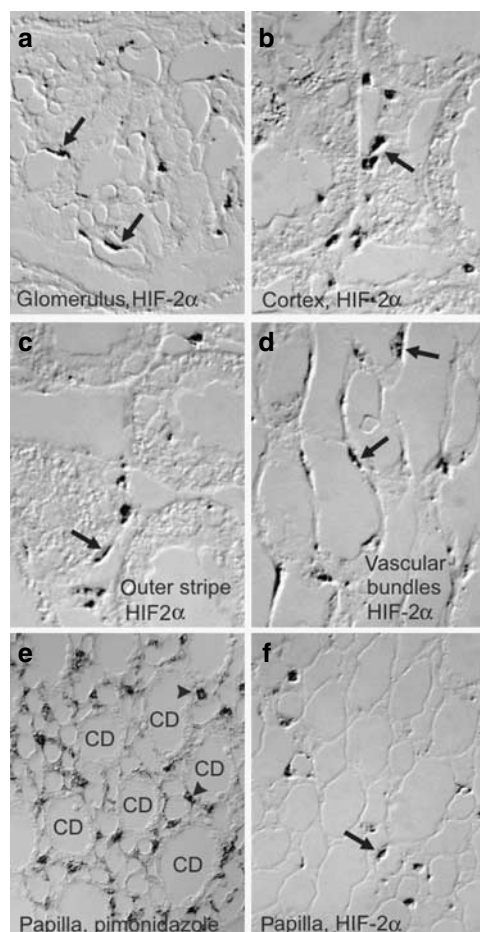


Figure 3 | Renal PIM and HIF-2 α induced by artificial Glc.

Immunohistochemistry for the hypoxia marker pimonidazole (PIM) and HIF-2 α ; arrow = endothelial cell and CD = collecting duct. Normal rats were studied after 2 h of artificial Glc. No signals for either marker were detected in CTRs, and no HIF-1 α signals were detected in Glc (not shown). Throughout the renal zones endothelial cells expressed HIF-2 α . In the cortex, glomeruli (a) and tubulointerstitial capillaries (b) stained positive. In the outer medulla, tubulointerstitial capillaries expressed HIF-2 α only in the outer stripe (c). By contrast, in the inner stripe, vascular bundles intensely stained for HIF-2 α , but the inter-bundle zone was void of signals (not shown). PIM, which only accumulate in deeply hypoxic tissue, were confined to the papillary interstitium (e; note that CDs are not stained). Accordingly, HIF-2 α was also expressed in the papilla (f). Magnification: $\times 1000$.

altered salt handling), which occur in STZ/CDS rats were responsible for this difference.

Factors which less likely had caused diabetic renal hypoxia include direct STZ toxicity³⁵ and hypovolemia.³³ Hypoxia developed over time in STZ and also occurred in CDS rats. Fluids had no impact on renal HIFs and PIM.

Declining tubular transport activity may explain the disappearance of PIM/HIF at 90 days of STZ. Noteworthy, in STZ, mTAL Na/K-ATPase activity (which may be considered a surrogate marker of oxygen consumption) is markedly increased at 35 days,³⁹ and normalizes or is even subnormal at 90 days^{39,40}, which well parallels the time course of renal hypoxia described in this study.

Table 4 | Changes at 24 h after delivery of CM to CTR and diabetic (14 days after STZ) rats

	Controls+CM (n=7)	Diabetes (STZ 14 days)+CM (n=6)
Animal weight (g)	339 \pm 7	297 \pm 14 ^a
Blood glucose (mg dl ⁻¹)	86 \pm 3	421 \pm 31 ^b
<i>Urine volume</i>		
0 day (ml h ⁻¹)	0.64 \pm 0.11	6.95 \pm 1.04 ^b
1 day	0.76 \pm 0.07	4.95 \pm 0.07 ^{b,c}
<i>PCr</i>		
0 day (μ mol l ⁻¹)	53 \pm 3	45 \pm 3
1 day	61 \pm 4	52 \pm 3
<i>Cl_{Cr}</i>		
0 day (ml min ⁻¹)	1.29 \pm 0.15	2.61 \pm 0.10 ^a
1 day	1.35 \pm 0.12	1.38 \pm 0.26 ^c
<i>Cl_{Cr} per 100 g</i>		
0 day (ml min ⁻¹)	0.37 \pm 0.05	0.83 \pm 0.04 ^d
1 day	0.39 \pm 0.03	0.45 \pm 0.08 ^c
<i>P-urea</i>		
0 day (mmol l ⁻¹)	6.7 \pm 0.5	13.7 \pm 2.1 ^d
1 day	8.6 \pm 2.1	12.4 \pm 2.5
<i>TRNa</i>		
0 day (%)	99.53 \pm 0.13	98.97 \pm 0.14 ^a
1 day	99.82 \pm 0.03	98.58 \pm 0.69
<i>FEK</i>		
0 day (%)	13.1 \pm 2.2	35.5 \pm 2.8 ^b
1 day	13.8 \pm 2.0	44.9 \pm 10.4 ^a

Cl_{Cr}, creatinine clearance; CM, contrast medium; CTR, control; FEK, fractional potassium excretion; PCr, plasma creatinine; STZ, streptozotocin; TRNa, tubular sodium reabsorption.

The effect of acute hypoxic insults on kidney function in controls (CTRs) and at 14 days of STZ. Both groups were subjected to meglumine iohalamate 8 ml kg⁻¹. ^a*P* < 0.05.

^b*P* < 0.001 vs CTR.

^c*P* < 0.05 vs baseline, non-paired, and paired *t*-test, respectively.

^d*P* < 0.01.

Table 5 | Renal papillary PIM, HIFs, and HO-1 at 1 and 2 h after delivery of contrast medium to CTR or diabetic (14 days after STZ) rats

	Control			Diabetes (STZ 14 days)		
	Untreated	CM (1 h)	CM (2 h)	Untreated	CM (1 h)	CM (2 h)
n=	5	3	9	13	3	9
Pimonidazole	0	2.0 \pm 0.0 ^a	0.3 \pm 0.3	1.7 \pm 0.3 ^a	3.3 \pm 0.3 ^b	2.7 \pm 0.3 ^b
HIF-1 α	0	1.7 \pm 0.3 ^a	0.9 \pm 0.2	1.5 \pm 0.2 ^a	3.0 \pm 0.6 ^b	2.8 \pm 0.2 ^b
HIF-2 α	0	1.7 \pm 0.3 ^a	0.7 \pm 0.2	1.4 \pm 0.2 ^a	3.3 \pm 0.3 ^c	2.8 \pm 0.3 ^d

CM, radiocontrast medium; CTR, control; HIF, hypoxia-inducible factor; STZ, streptozotocin.

Semiquantitative immunohistochemical staining: 0, no signals detectable; 1+, staining in <5% of tubular profiles or interstitial/endothelial cells; 2+, 5–20%; 3+, 20–33%; 4+, 33–50%. In both control and diabetic animals, location of signals followed the same renal zone-specific pattern described in Table 3.

^a*P* < 0.01 vs untreated controls.

^b*P* < 0.001.

^c*P* < 0.01.

^d*P* < 0.05 vs untreated diabetics, ANOVA.

Different hypoxia patterns in diabetes and artificial Glc

As mentioned above, Glc lead to renal PIM/HIF appearance, albeit with a pattern largely different from STZ/CDS rats. In the latter PIM/HIFs mainly located in the inter-bundle zone of the inner stripe, at the site of high tubular reabsorptive activity, suggesting a major contribution of tubular workload. By contrast, Glc seems to primarily induce endothelial stress, since vascular bundles of the inner stripe intensely stained for HIF-2 α , but no signals were detectable in the inter-bundle zone. We have no explanation for this particular distribution of HIF-2 α immunoreactivity, that might be triggered by factors other than hypoxia *per se*, as previously shown by studies in cell cultures kept under 21% ambient oxygen.^{41,42} However, such normoxic HIF activation would take much longer than 2 h, since it is based on enhanced HIF α transcription/translation. By contrast, hypoxic HIF activation through blockade of HIF α proteolysis is almost instantaneous. Moreover, PIM adducts shown in the papilla during Glc indicate that, indeed, hypoxia played a role in endothelial HIF activation.

Tempol augments hypoxia response *in vivo*

Generation of O₂⁻ is an attractive explanation for diabetes-induced renal hypoxia, since O₂⁻ is activated in diabetes,²² promotes renal medullary vasoconstriction,²⁴ and enhances tubular reabsorptive activity.²⁵ In this study there was a trend ($P=0.075$) for reduced PIM staining with tempol, which with a higher N (number of animals) might have reached statistical significance.

The impact of ROS on HIF activity is a matter of debate, given that *in vitro* studies have provided conflicting results.^{18–21} Yang *et al.*²⁶ have shown that O₂⁻ reduces HIF-1 α and its target gene HO-1 in renal medullary interstitial cells, which could be prevented by tempol. Katavetin *et al.*⁴³ demonstrated that D-glucose blunted the hypoxia response in immortalized rat proximal tubular cells, which could be prevented by the radical scavenger α -tocopherol. Zou and Cowley²¹ have nicely reviewed the current knowledge about HIF/O₂⁻ interaction, supporting the view that O₂⁻ reduces hypoxic HIF activation, probably through an increased proteasomal degradation of HIF α . To our knowledge, the impact of ROS on HIF has not been addressed *in vivo*, so far. In concordance with the view of Zou and Cowley we show that tempol augments HIFs and HO-1 *in vivo* in the diabetic renal medulla, suggesting that local production of O₂⁻ may have suppressed HIFs.

CM aggravates renal hypoxia in diabetes

Diabetics are prone to develop CM-induced AKI,^{8,9} but the underlying mechanisms are largely unknown. Hypoxia has been proposed as a unifying hypothesis in AKI, and particularly so in radiocontrast nephropathy.^{29,34} In support of this view, we show for the first time that CM leads to intensified and protracted renal hypoxia in diabetic rats. Moreover, we demonstrate that, at least in early stages of diabetes, CM also enhances renal HIFs, suggesting hypoxia

adaptation. Such adaptive responses may, at least partly, explain that in our study morphology was preserved at 24 h after CM, despite some functional impairment. One could speculate that in more advanced experimental or human diabetic nephropathy, the potential for hypoxia adaptation would be reduced, and consequently, overt CM-induced cell damage would occur.

CONCLUSIONS

Experimental diabetes leads to transient renal medullary hypoxia, which is largely dependent on Glc. Intensified and protracted hypoxia following CM is a possible explanation for the propensity to CM-induced AKI in diabetes. Nevertheless, diabetic kidneys hold a potential for HIF-mediated cell protection, and its enhancement might be a logical therapeutic strategy in the prevention of AKI and in ameliorating the progression of tubulointerstitial disease in the diabetic kidney.

MATERIALS AND METHODS

Animals and materials

Male SD rats (250–350 g) were used for the STZ model (of insulin-deficient diabetes with both fasting and PP Glc) and artificial Glc studies detailed below, fed regular chow and with free access to water. Inbred CDS rats were used as an attenuated model of insulin deficient diabetes, with normal fasting insulin and blood glucose levels, but protracted PP Glc due to deficient β -cell response.^{44,45}

Chemicals were purchased from Sigma (St Louis, MO), if not stated otherwise. Experiments were conducted in accordance with the NIH Guidelines for the Care and Use of Laboratory Animals.

Experimental groups

STZ-induced diabetic rats, a model of partial type I diabetes: SD rats received a single intraperitoneal injection of freshly prepared STZ (65 mg kg⁻¹ body weight, dissolved in 100 mmol l⁻¹ citric acid, pH 4.5), and confirmed 2 days later by PP blood glucose (>250 mg dl⁻¹).

CTR rats: Vehicle-injected SD rats after 2 to 7 days, 14 to 30 days, and 90 days served as CTR for the 2 and 7 days STZ, the 14 and 30 days STZ, and for the 90 days STZ, respectively.

Insulin treatment in STZ: Glc was normalized in seven animals during 12–14 days of STZ by subcutaneous insulin implants (2U day⁻¹; Lin Shin Canada, Ontario, Canada).

Anti-oxidant treatment in STZ: According to Li⁴⁶ the soluble superoxide dismutase mimetic 4-hydroxyl-tetramethylpiperidin-oxyl (tempol, kindly provided by Haj Yechia⁴⁷) was added to drinking water (about 120 mg kg⁻¹ day⁻¹) from 2 to 14 days of STZ.

Fluid replacement: 14-day STZ diabetic rats were given two 4 ml saline injections intraperitoneally, 1 h apart, and were killed 1 h later for immunohistochemistry. PIM was injected intravenously concomitantly with the second intraperitoneal fluid load.

CDS model: CDS rats 6- to 8-week old, initially weighing 240–280 g, were studied after an interval of 30 days on a special copper-free diabetogenic diet (18% casein, 72% sucrose, 4.5% butter, 0.5% corn oil, 5% salt No II USP, and fat-soluble vitamins, distilled water *ad libitum*). Of note, this diet is a prerequisite for the development of the diabetic phenotype, characterized by normal fasting glucose but protracted PP Glc.^{44,45} Animals were trained to eat in the morning, and assessment of glycemia and renal harvesting

for immunostaining were carried out 2–3 h after a documented morning snack.

Short-term artificial hyperglycemia (Glc): hyperglycemia (Glc) ($>250 \text{ mg dl}^{-1}$) was induced in SD rats according to the procedure described by Lien;⁴⁸ inactin anesthesia (100 mg kg^{-1}), intravenous infusion of 10% glucose coupled with the somatostatin analogue octreotide (Sandoz Pharma, Basel, Switzerland; $10 \mu\text{g}$ bolus followed by $1 \mu\text{g min}^{-1}$ infusion). Glc was maintained for 2 h and validated at 30-min intervals.

CM-induced acute renal hypoxia in CTR and at 14 and 30 days of STZ: In a separate set of experiments, following a baseline period in metabolic cages, under anesthesia (ketamine 100 mg kg^{-1} intraperitoneally) the femoral artery was cannulated with a polyethylene tube (PE-50; Clay-Adams, Parsippany, NJ), and the animals were subjected to the CM meglumine iohalamate (Conray 60%; Mallinckrodt, St Louis, MO; 6 ml kg^{-1} intra-arterial). The vascular catheters were removed and the rats were killed for immunohistochemistry at 1 or 2 h later (only at 14 days of STZ), or were allowed to recover in metabolic cages and killed 24 h later for renal morphology or immunohistochemistry. Mortality (by 24 h) among STZ and CTR subjected to CM was 2 and 0%, respectively. CTR groups used in these series were weight-matched for the 14-day period (to ensure comparable radiocontrast volume) and age-matched for the 30-day period.

Functional studies and the renal perfusion fixation technique

Rats were kept in metabolic cages (Nalge, Rochester, NY) for 24 h. Under pentobarbital anesthesia (60 mg kg^{-1}) the kidneys were perfusion-fixed selectively through the abdominal aorta, with 1.25% glutaraldehyde (for semi-thin sections) or with 3% paraformaldehyde (for immunohistochemical studies), as previously detailed.^{30,49} The weight of the two kidneys was determined following the fixation perfusion. Plasma and urine samples were processed for the determination of creatinine, urea, sodium, and potassium, and creatinine clearance, fractional sodium reabsorption, and potassium excretion were calculated.

Determination of renal morphology

Kidney slices were postfixed in buffered 2% OsO_4 , dehydrated, and embedded in an Araldite-EM bed 812 mixture. Large sections were cut perpendicular to the renal capsule, containing cortex, and medulla. Thin ($1 \mu\text{m}$) sections were analyzed in a blinded manner for morphological alterations, as previously detailed.⁴⁹

Determination of renal parenchymal hypoxia and potential hypoxia adaptation

Renal hypoxia and hypoxia adaptation were assessed by immunostaining for pimonidazole (Hypoxyprobe, Pharmacia International, Belmont, MA; PIM), HIFs, and heme-oxygenase-1 (HO-1).^{29,30} PIM, which binds to tissues with pO_2 levels below 10 mm Hg ,^{50,51} was injected *in vivo* (60 mg kg^{-1} intravenously) 1 h before the kidneys were perfusion fixed. The following primary antibodies were used as previously reported:^{29–32} mouse anti-human HIF-1 α ($\alpha 67$; Novus Biologicals, Littleton, CO; 1:10 000), rabbit anti-mouse HIF-2 α (PM9, gift from Patrick Maxwell, Hammersmith Hospital, Imperial College, London, UK; 1:10 000), rabbit anti-rat HO-1 (Stressgen, Victoria, Canada; 1:60 000), mouse anti-pimonidazole (Hypoxyprobe; Natural Pharmacia International, Belmont, MA; 1:1000). Immunostaining was assessed semiquantitatively on a 0 to 4+ score basis: 0, no signals detectable; 1+, staining in $<5\%$ of tubular profiles or interstitial/endothelial cells; 2+, 5–20%; 3+, 20–33%; and 4+, 33–50%.

Statistics

Data are represented as means \pm s.e.m. Student's *t*-test and multiple comparisons with *t*-test *post hoc* analysis of variance were used as indicated below, for the comparison of morphological, immunohistological and functional parameters. Statistical significance was set at $P < 0.05$.

ACKNOWLEDGMENTS

This work, formerly presented in part in abstract forms (*J Am Soc Nephrol* 15:468A, 2004; *J Am Soc Nephrol* 16:402A, 2005), was supported by the Russell Berrie Foundation and D-Cure, Diabetes Care in Israel, by the Harvard Medical Faculty Physicians at Beth Israel Deaconess Medical Center, Boston, MA, and by the Open Nephrology Science Centre, Berlin, Germany.

REFERENCES

- Hochachka PW, Buck LT, Doll CJ, Land C. Unifying theory of hypoxia tolerance: molecular/metabolic defense and rescue mechanisms for surviving oxygen lack. *Proc Natl Acad Sci USA* 1996; **93**: 9493–9498.
- Palm F, Cederberg J, Hansell P *et al*. Reactive oxygen species cause diabetes-induced decrease in renal oxygen tension. *Diabetologia* 2003; **46**: 1153–1160.
- Ries M, Basseau F, Tyndal B *et al*. Renal diffusion and BOLD MRI in experimental diabetic nephropathy. Blood oxygen level-dependent. *J Magn Reson Imaging* 2003; **17**: 104–113.
- Eckardt KU, Bernhardt WM, Weidemann A *et al*. Role of hypoxia in the pathogenesis of renal disease. *Kidney Int Suppl* 2005; **99**: S46–S51.
- Rosenberger C, Rosen S, Heyman SN. Intrarenal oxygenation in acute renal failure. *Clin Exp Pharmacol Physiol* 2006; **33**: 980–988.
- Nangaku M. Chronic hypoxia and tubulointerstitial injury: a final common pathway to end stage renal failure. *J Am Soc Nephrol* 2006; **17**: 17–25.
- Griffin MD, Bergstralhn EJ, Larson TS. Renal papillary necrosis—a sixteen-year clinical experience. *J Am Soc Nephrol* 1995; **6**: 248–256.
- Rudnick MR, Goldfarb S, Wexler L *et al*. Nephrotoxicity of ionic and nonionic contrast media in 1196 patients: a randomized trial. The Iohexol Cooperative Study. *Kidney Int* 1995; **47**: 254–261.
- McCullough PA, Wolyn R, Rocher LL *et al*. Acute renal failure after coronary intervention: incidence, risk factors, and relationship to mortality. *Am J Med* 1997; **103**: 368–375.
- Thakar CV, Arrigain S, Worley S *et al*. A clinical score to predict acute renal failure after cardiac surgery. *J Am Soc Nephrol* 2005; **16**: 162–168.
- Rosner MH, Okusa MD. Acute kidney injury associated with cardiac surgery. *Clin J Am Soc Nephrol* 2006; **1**: 19–32.
- Jones CA, Krolewski AS, Rogus J *et al*. Epidemic of end-stage renal disease in people with diabetes in the United States population: do we know the cause? *Kidney Int* 2005; **67**: 1684–1691.
- Maxwell PH. HIF-1's relationship to oxygen: simple yet sophisticated. *Cell Cycle* 2004; **3**: 156–159.
- Metzen E, Ratcliffe PJ. HIF hydroxylation and cellular oxygen sensing. *Biol Chem* 2004; **385**: 223–230.
- Semenza GL. Hydroxylation of HIF-1: oxygen sensing at the molecular level. *Physiology* 2004; **19**: 176–182.
- Rosenberger C, Rosen S, Heyman S. Current understanding of HIF in renal disease. *Kidney Blood Press Res* 2005; **28**: 325–340.
- Arjamaa O, Nikinmaa M. Oxygen-dependent diseases in the retina: role of hypoxia-inducible factors. *Exp Eye Res* 2006; **83**: 473–483.
- Pouyssegur J, Mechta-Grigoriou F. Redox regulation of the hypoxia-inducible factor. *Biol Chem* 2006; **387**: 1337–1346.
- Kaelin Jr WG. ROS: really involved in oxygen sensing. *Cell Metab* 2005; **1**: 357–358.
- Kietzmann T, Gorch A. Reactive oxygen species in the control of hypoxia-inducible factor-mediated gene expression. *Semin Cell Dev Biol* 2005; **16**: 474–486.
- Zou AP, Cowley Jr AW. Reactive oxygen species and molecular regulation of renal oxygenation. *Acta Physiol Scand* 2003; **179**: 233–241.
- Fridlyand LE, Philipson LH. Oxidative reactive species in cell injury: mechanisms in diabetes mellitus and therapeutic approaches. *Ann N Y Acad Sci* 2005; **1066**: 136–151.
- Li N, Yi FX, Spurrier JL *et al*. Production of superoxide through NADH oxidase in thick ascending limb of Henle's loop in rat kidney. *Am J Physiol Renal Physiol* 2002; **282**: F1111–F1119.

24. Zou AP, Li N, Cowley Jr AW. Production and actions of superoxide in the renal medulla. *Hypertension* 2001; **37**: 547–553.
25. Juncos R, Garvin JL. Superoxide enhances Na–K–2Cl cotransporter activity in the thick ascending limb. *Am J Physiol Renal Physiol* 2005; **288**: F982–F987.
26. Yang ZZ, Zhang AY, Yi FX *et al*. Redox regulation of HIF-1 α levels and HO-1 expression in renal medullary interstitial cells. *Am J Physiol Renal Physiol* 2003; **284**: F1207–F1215.
27. Banday AA, Marwaha A, Tallam LS, Lokhandwala MF. Tempol reduces oxidative stress, improves insulin sensitivity, decreases renal dopamine D1 receptor hyperphosphorylation, and restores D1 receptor–G-protein coupling and function in obese Zucker rats. *Diabetes* 2005; **54**: 2219–2226.
28. Abraham NG, Kappas A. Heme oxygenase and the cardiovascular–renal system. *Free Radic Biol Med* 2005; **39**: 1–25.
29. Rosenberger C, Heyman SN, Rosen S *et al*. Upregulation of HIF in experimental acute renal failure: evidence for a protective transcriptional response to hypoxia. *Kidney Int* 2005; **67**: 531–542.
30. Rosenberger C, Griethe W, Gruber G *et al*. Cellular responses to hypoxia after renal segmental infarction. *Kidney Int* 2003; **64**: 874–886.
31. Rosenberger C, Rosen S, Shina A *et al*. Hypoxia inducible factors and tubular cell survival in isolated perfused kidneys. *Kidney Int* 2006; **70**: 60–70.
32. Rosenberger C, Mandriota S, Jürgensen JS *et al*. Expression of hypoxia-inducible factor-1 α and -2 α in hypoxic and ischemic rat kidneys. *J Am Soc Nephrol* 2002; **13**: 1721–1732.
33. Manotham K, Tanaka T, Ohse T *et al*. A biologic role of HIF-1 in the renal medulla. *Kidney Int* 2005; **67**: 1428–1439.
34. Prasad PV, Priatna A, Spokes K, Epstein FH. Changes in intrarenal oxygenation as evaluated by BOLD MRI in a rat kidney model for radiocontrast nephropathy. *J Magn Reson Imaging* 2001; **13**: 744–747.
35. Kraynak AR, Storer RD, Jensen RD *et al*. Extent and persistence of streptozotocin-induced DNA damage and cell proliferation in rat kidney as determined by *in vivo* alkaline elution and BrdUrd labeling assays. *Toxicol Appl Pharmacol* 1995; **35**: 279–286.
36. Epstein FH, Silva P, Spokes K *et al*. Renal medullary Na–K–ATPase and hypoxic injury in perfused rat kidneys. *Kidney Int* 1989; **36**: 768–772.
37. Ward DT, Yau SK, Mee AP *et al*. Functional, molecular, and biochemical characterization of streptozotocin-induced diabetes. *J Am Soc Nephrol* 2001; **12**: 779–790.
38. Leyssac PP, Holstein-Rathlou N-H, Skott O. Renal blood flow, early distal sodium, and plasma renin concentrations during osmotic diuresis. *Am J Physiol Regul Integr Comp Physiol* 2000; **279**: R1268–R1276.
39. Wald H, Scherzer P, Rasch R, Popovtzer MM. Renal tubular Na(+)-K(+)-ATPase in diabetes mellitus: relationship to metabolic abnormality. *Am J Physiol* 1993; **265**: E96–E101.
40. Tsimaratos M, Coste TC, Djemli-Shipkolye A *et al*. Gamma-linolenic acid restores renal medullary thick ascending limb Na(+), K(+)-ATPase activity in diabetic rats. *J Nutr* 2001; **131**: 3160–3165.
41. Haddad JJ, Harb HL. Cytokines and the regulation of the hypoxia-inducible factor (HIF)-1 α . *Int Immunopharmacol* 2005; **5**: 461–483.
42. Zhou J, Fandrey J, Schümann J *et al*. NO and TNF- α release from activated macrophages stabilize HIF-1 α in resting tubular LLC-PK1 cells. *Am J Physiol* 2003; **284**: C439–C446.
43. Katavetin P, Miyata T, Inagi R *et al*. High glucose blunts vascular endothelial growth factor response to hypoxia via the oxidative stress-regulated hypoxia-inducible factor/hypoxia-responsible element pathway. *J Am Soc Nephrol* 2006; **17**: 1405–1413.
44. Yagil H, Barak A, Ben-Dor D *et al*. Nonproteinuric diabetes-associated nephropathy in the Cohen rat model of type 2 diabetes. *Diabetes* 2005; **54**: 1487–1496.
45. Weksler-Zangen S, Yagil H, Zangen DH *et al*. The newly inbred cohen diabetic rat. A non-obese normolipidemic genetic model of diet-induced type 2 diabetes expressing sex differences. *Diabetes* 2001; **50**: 2521–2529.
46. Li J, Chen YJ, Quilley J. Effect of tempol on renal cyclooxygenase expression and activity in experimental diabetes in the rat. *J Pharmacol Exp Ther* 2005; **314**: 818–824.
47. Nassar T, Kadery B, Lotan H *et al*. Effects of the superoxide dismutase-mimetic compound tempol on endothelial dysfunction in streptozotocin-induced diabetic rats. *Eur J Pharmacol* 2002; **436**: 111–118.
48. Lien EL, Garsky VM. Route of administration as a factor in the selectivity of hormone suppression of a somatostatin analogue in rats. *Horm Metab Res* 1981; **13**: 675–678.
49. Goldfarb M, Rosenberger C, Abassi Z *et al*. Acute-on-chronic renal failure in the rat: functional compensation and hypoxia tolerance. *Am J Nephrol* 2006; **26**: 22–33.
50. Franko AJ, Chapmann JD. Binding of 14C-misonidazole to hypoxic cells in V79 spheroids. *Br J Cancer* 1982; **45**: 694–699.
51. Arteel GE, Thurmann RG, Raleigh JA. Reductive metabolism of the hypoxia marker pimonidazole is regulated by oxygen tension independent of the pyridine nucleotide redox state. *Eur J Biochem* 1998; **253**: 743–750.